DOI: 10.1002/adma.201801169

Article type: Communication

Polymethacrylamide and Carbon Composites that Grow, Strengthen and Self-Repair using Ambient Carbon Dioxide Fixation

Seon-Yeong Kwak[1], Juan Pablo Giraldo[2], Tedrick T. S. Lew[1], Min Hao Wong[1], Pingwei Liu[1], Yun Jung Yang[1], Volodymyr B. Koman[1], Melissa K. McGee[1], Bradley D. Olsen[1], Michael S. Strano[1,*]

Dr. S.-Y. Kwak, T.T.S. Lew, M.H. Wong, Dr. P. Liu, Dr. Y.J. Yang, Dr. V.B. Koman, M.K. McGee, Prof. B.D. Olsen, Prof. M.S. Strano

Chemical Engineering

Massachusetts Institute of Technology

Cambridge, MA 02139, USA

Prof. J.P. Giraldo

Botany and Plant Sciences

University of California Riverside

Riverside, CA 92507 USA

Keywords: carbon fixating materials, chloroplast-embedded hydrogels, self-repairing, ambient CO_2 fixation, polymethyacrylamide and carbon composites

Plants accumulate solid carbon mass and self-repair using atmospheric CO_2 fixation from photosynthesis. Synthetic materials capable of mimicking this property can significantly reduce the energy needed to transport and repair construction materials. Here, we demonstrate that a gel matrix containing aminopropyl methacrylamide (APMA), glucose oxidase (GOx) and nanoceria stabilized-extracted chloroplasts is able to grow, strengthen and self-repair using carbon fixation. Glucose produced from the embedded chloroplasts is converted to gluconolactone (GL) via GOx, polymerizing with APMA to form a continuously expanding and strengthening polymethacrylamide. We show extracted spinach chloroplasts exhibit enhanced stability and produce 12 μg of GL mg^{-1} Chl h^{-1} by optimization of the temporal illumination conditions, insertion of chemoprotective nanoceria inside the chloroplasts, and increasing the glucose efflux rate. This system achieves an average growth rate of 60 μm^3 h^{-1} per chloroplast under ambient CO_2 and illumination over 18 hours, thickening with a shear modulus of 3 kPa. This material can demonstrate self-repair using the exported glucose from chloroplasts and chemical crosslinking through the fissures. These results point to a new class of materials capable of using atmospheric CO_2 fixation as a regeneration source, finding utility as self-healing coatings, construction materials, and fabrics.

Materials capable of dynamic self-repair are commonly found among living scaffolds and tissues. Correcting damage through self-repair mechanisms promise enhanced material lifetimes and increased resistance from fatigue and acute mechanical stress. There has been a concerted research effort to develop synthetic materials mimicking aspects this natural property by dynamic chemistry based on either covalent bonds or non-covalent interactions that form or break reversibly.[1-11] However, an important distinction can be made here.

These dynamic chemical approaches necessarily require one or more external stimuli such as heating, pH, mechanical stress, UV light, and external chemical treatment.[1-3] Alternatively, autonomous systems, defined as materials that themselves can detect and respond to damage, have been recently introduced. An *encapsulated-monomer* approach was first reported by White and co-workers in 2001,[12] in which reservoirs of a monomer and a polymerization initiator or catalyst are contained within the bulk of the material.[13,14] A variant approach using bacteria (*Bacillus Sphaericus*)-induced carbonate precipitation was utilized for micro-cracks healing on a concrete material, but bacteria action was limited due to lack of the local energy sources and low survivability in concrete.[15] The energy source limitation may in-fact translate into a fundamental one for the use of heterotrophic living organisms in materials.

Herein, we define what we identify as a new direction in self-healing materials as combining the autonomy of damage response with the ability to exceed the material's own local material balance. To this end, we create a novel class of material designed to grow, repair and strengthen through carbon fixation. We accomplish this by using embedded, extracted chloroplasts as carbon-fixing photocatalysts, which utilize abundant atmospheric CO_2 and solar energy (**Figure 1**) as drivers. We design the chemistry of material synthesis to use glucose, a saccharide exported from chloroplasts, for facile reaction under relatively mild conditions. Several strategies are systematically investigated to improve glucose export from isolated chloroplasts, shown to be the limiting factor in the growth and repair rate of the material. The exported glucose is converted to GL, which subsequently reacts with primary amine-functionalized acrylamide monomers, 3-aminopropyl methacrylamide (APMA), to build a polymer matrix. We demonstrate this chloroplast embedded-gel matrix, containing

lightly cross-linked polymer networks that swell in water, continually grows, strengthens, and self-repairs using fixation of atmospheric CO_2 as a regeneration source under ambient illumination.

Hydrogel Composite Design and Synthesis

The three major saccharides exported from chloroplasts (extracted or in-vivo) are maltose, glucose and triose phosphate.[16] We selected glucose as a reagent to focus on because it is easily converted into a reactive precursor, gluoconolactone (GL). One D-glucose molecule is oxidized to one D-gluocono-1,5-lactone molecule and one hydrogen peroxide (H_2O_2) molecule by glucose oxidase (GOx). These scheme has been used for glycopolymer synthesis previously.[17-20] The product of the polymerization reaction of GL and aminopropyl methacrylamide (APMA) appears transparent and gel-like. The characteristic IR peaks, lactone C=O of GL appears at 1719.7 cm^{-1} and acrylamide C=O of APMA appears at 1652.9 cm^{-1} and 1616.7 cm^{-1} in the mixture of GL and APMA at 0 h (**Figure 2**A, S1 and S2). The mixture of GL and APMA in pH 7.0 phosphate buffer is put under the ambient light for 5 h until hydrogel (denoted as GPMAA) forms, as indicated by the presence of a new broad peak at 1624.3 cm^{-1} that corresponds to the formation of amide bond between GL and APMA as well as the polymerization of acrylamide (Figure 2A). The rheological properties of the hydrogels show that the storage modulus G' at high angular frequency (100 rad s^{-1}) is 3 kPa and shear modulus measured at different reaction times implies that GPMAA synthesis in completed within 18 h (Figure 2B and S3). GPMAA shows a swelling property and exhibits a 115-fold increase hydrogel weight in 48 h due to water absorption. Using atomic force

microscopy as an indenter, the Young's modulus of chloroplasts was estimated to be 26 (±5) kPa,[21] which is higher than that of the swollen GPMAA hydrogel (water 50 wt%) at 8.2 (±4.1) kPa and lower than that of dry GPMAA at 348 (±125) kPa (Figure S5). Thus, we expect that the chloroplasts can reinforce the GPMAA hydrogel in a liquid environment. In addition, we find that graphene oxide at low weight fraction (0.01 wt%) can be used to immobilize glucose oxidase (GOx) on the surface of graphene oxide sheets, which also serve as mechanical inclusions for stiffening.[22-24] Graphene oxide-containing hydrogel is formed within 6 h, which is 3 times faster than that of hydrogel formation without graphene oxide (Figure 2C). After 6 h, the shear modulus of GPMAA hydrogel is 0.4 (± 0.05) kPa while that of graphene oxide containing GPMAA hydrogel is 3.5 (± 0.19) kPa, which is approximately 9 times higher. The shear modulus of GPMAA hydrogel at 18 h (completely formed) is 3.0 (± 0.087) kPa, which is still approximately 17% lower than that of graphene oxide containing GPMAA. We observed that such a low fraction of graphene oxide could stiffen hydrogel 3 times faster by accelerating crosslinking, enhancing the mechanical strength by 17% as the composite material is intertwined by hydrogen bonds between hydroxyl and epoxy groups of graphene oxide sheets and GPMAA chains (Figure 2B and S4).[25] The hydrogel exhibits adhesive properties, which displays characteristic fibrillar structure and shear strength profile during the separation process (Figure 2C and 2D) and can hold the weight of 12 mL of water in a centrifugal tube (Figure S6).

Engineering of Extracted Spinach Chloroplasts

Since glucose export from the extracted chloroplasts is a potential rate-limiting step in material growth, this prompted an optimization study on glucose export. Chloroplasts, plant organelles contained within the cytoplasm of the plant cell, are the main sites of carbon fixation and photosynthesis in plants. They have been explored as candidates for solar energy generation and efficient carbon dioxide sequestration (100 μmol CO_2 mg^{-1} Chl h^{-1}) due to their inherent ability to export stored chemical energy,[26,27] abundance in nature, and scalable isolation from plant matter.[28] However, they have not been used as components within materials. Exported sugars ultimately participate in the sucrose synthetic pathway through a series of enzymatic reactions in the cytoplasm of protoplasts.[29] This pathway is absent in isolated chloroplast, potentially yielding accumulation of exported glucose and increased availability for material synthesis. Therefore, extracted chloroplasts can accumulate exported saccharides with the absence of the sucrose synthetic route.

We explored several biochemical and nano-biotechnological approaches to increase the export rate of glucose from isolated chloroplasts. Under dark conditions, maltose and glucose are the major sugars exported from chloroplasts.[16] Maltose is a disaccharide consisting of two glucose molecules joined with a α(1→4) glycosidic bond that α–glucosidase can hydrolyze. Therefore, we explored the use of α–glucosidase in the chloroplast incubation medium as a means of converting the maltose to glucose and boosting the glucose yield. We observe that the glucose concentration outside of the extracted chloroplast after 2 h of light and 2 h of dark period with α–glucosidase is about 3 times higher than that of control without α–glucosidase (**Figure 3**A). This proves that the maltose is exported from the chloroplast

and subsequently broken down by enzymatic hydrolysis to produce additional glucose molecules for eventual polymerization.

Starch formation and sucrose synthesis are often viewed as competitive processes since starch is formed in the chloroplasts by photosynthesis during the day and exported after being broken down to synthesize sucrose at night.[16,30-35] Indeed, glucose concentration significantly declines under continuous illumination for 24 h without an intermittent dark period (Figure 3B). This appears consistent with the starch degradation process becoming latent or a glucose influx competitively operating with glucose export.[30] Alternatively, if stored in the dark for 24 h, chloroplasts equilibrate glucose to a constant concentration (Figure 3B), which supports the conclusion that a prior period of illumination is necessary before a dark period for starch formation, breakdown and glucose export.

Another important variable is inorganic phosphate (Pi) concentration. It is known to play a key role in photosynthesis and carbon metabolism.[36-38] The photosynthesis of isolated chloroplasts soon ceases in the absence of Pi but restarts with exogenous addition of Pi to the medium.[39] Consequently, we hypothesize that a Pi deficiency can limit carbon export from isolated chloroplasts. To investigate the importance of external Pi concentration on glucose export, isolated chloroplasts are incubated in buffer containing 5 mM Pi, with subsequent hourly additions of Pi to the incubation medium to maintain an external Pi concentration. However, we see an insignificant difference in external glucose concentration with this high Pi supply as shown in Figure 3B. We conclude that supplying external Pi is not an effective strategy to increase the glucose export rate in extracted chloroplasts.[16]

The membrane mechanisms for glucose export can also equilibrate with an influx rate, leading to limiting glucose concentrations outside the chloroplast.[35,40] As another optimization variable, we adjusted the pH of the chloroplast suspension from pH 7.6 to pH 8.0 to mimic the proton gradient between the chloroplast stroma and the external environment in the dark.[40] Figure 3C shows that the change in glucose concentration is negligible and within the error range even with the introduction of external adenosine triphosphate (ATP) to induce the active transport of glucose in the presence of 5 mM Pi.[33] To minimize glucose influx and increase glucose export, we continually lowered the external glucose concentration by converting glucose to glucose-6-phosphate by hexokinase. This results in an increase of glucose export at a rate of approximately 5 μg mg^{-1} Chl h^{-1} in the dark period (Figure 3D). In a biological system, negative feedback is a well-known regulatory mechanism in which the formation of a product in turn reduces the driving force for its own production. However, to the best of our knowledge, this is the first demonstration of boosting the net glucose export from isolated chloroplasts by adjusting the glucose gradient across the chloroplast membrane. As expected, additional Pi results in insignificant enhancement of glucose export from isolated chloroplasts.

Stabilization through Plant Nanobionics

Chloroplasts outside of the plant cells have limited photoactive lifetimes of less than a day and only a few hours for saccharide export.[16,33] Several strategies have been attempted to extend chloroplast photostability, for example by encapsulating chloroplast in biologically

inert matrices and altering conditions such as illumination, temperature, and buffer composition.[41,42] Previously, our group showed that potent antioxidant cerium oxide nanoparticles, nanoceria, could extend the photoactive lifetime of isolated chloroplasts by scavenging reactive oxygen species (ROS) produced as a by-product of photosynthesis.[43,44] However, the effect of ROS scavenging on glucose export remained unknown. We hypothesize that the protection of the carbon export system from ROS-related degradation or photodamage can help maintain high carbon export rates for a longer period of time. Isolated chloroplasts are first pre-incubated with nanoceria to allow the nanoparticles to enter the chloroplasts as we have shown previously.[44] After the incubation, the buffer was replaced with a fresh buffer without nanoceria and the chloroplast suspension is illuminated for 4 h and subsequently kept in the dark for 4 h. To boost glucose export, we added hexokinase every hour during the dark period. An insignificant effect on glucose export is observed at both low (5 μM, 0.56 mg L^{-1}) and high (50 μM, ~5.6 mg L^{-1}) concentration of nanoceria (Figure S7A). When we extend the light period from 4 h to 12 h, 50 μM nanoceria gives a positive effect on glucose export after 6 h from the start of dark period, while a marginal improvement is observed at 5 μM (Figure 3E). We conclude that removing photo-generated ROS inside chloroplasts can extend the lifetime of isolated chloroplasts, which ultimately translates into higher glucose accumulation in the medium. We also note that glucose export increases only after the addition of hexokinase, which acts as a sink for this flux outside of the chloroplast.

In all, the yield of glucose can be increased using enzymatic hydrolysis of maltose exported from isolated chloroplasts. We observe a net increase in glucose export by

adjusting the glucose gradient across the chloroplast membrane, optimizing the illumination period and enhancing the photo-stability of chloroplasts. We apply our findings to boost glucose export from isolated chloroplasts with the ultimate goal of conversion to the monomer, GL. Similar to the regulation of glucose equilibrium across the chloroplast membrane by hexokinase (Figure 3D), the conversion reaction of external glucose to GL by GOx promotes glucose export by suppressing glucose accumulation in the medium (Figure 3F). In the presence of 20 U mL^{-1} GOx, the GL concentration notably increases at a rate of 12 µg mg^{-1} Chl h^{-1} whereas the lower (10 U mL^{-1}) concentration of GOx leads to negligible improvement in the glucose export rate (Figure 3F). We observe that this increase reaches to a plateau within a few hours and the GL concentration barely increases in higher GOx (50-100 U mL^{-1}) (Figure S7B). The fast accumulation of H_2O_2 from GOx enzymatic catalysis may contribute to this saturation. In the presence of high H_2O_2 concentration, CO_2 fixation ceases or its rate significantly diminishes since H_2O_2 and CO_2 both compete for photoreductants generated in the thylakoids of chloroplasts.[46] From the continuous increase of GL during the illuminated period, we discover that glucose gradient adjustment across the membrane is the more critical variable that affects glucose export than manipulating the light/dark cycle (Figure S7C). This brings huge benefits to the chloroplast-embedded hydrogel growth since photosynthesis, glucose export and conversion, and polymerization can occur all together under the illumination.

Carbon Fixation in the Hydrogel System

Putting these components together, we construct a material that autonomously grows, strengthens and repairs itself in response to certain types of damage. We pre-incubate isolated chloroplasts with 50 μM nanoceria for 3 h at 4 ˚C to prolong their lifetime, and then replace the nanoceria solution with buffer containing both APMA and GOx. It is critical to purge the remaining nanoceria from the medium because photogenerated free radicals are mechanistically essential to the polymerization and crosslinking process. We find that isolated chloroplasts function well in media containing up to 0.1% w/v APMA but show significantly lower glucose export rates at 0.4% w/v APMA (Figure S9). GOx has been demonstrated to maintain its catalytic activity over that period.[46] Within 6 h from the start of the illumination period, hydrogel-like material can be observed around the chloroplast membrane. After 18 h, the hydrogel has clearly extended to a thickness of more than 20 μm and the chloroplasts become gradually embedded in the hydrogel (**Figure 4**A and S10). When the mean concentration of glucose in the medium is 5 μM, the estimated glucose concentration near the chloroplast outer membrane is approximately 125 mM within a 100 nm distance. Therefore, our experimental results show that hydrogel forms mostly around the chloroplast membranes rather than in non-specific locations in the medium. When we immobilize GOx on the surface of graphene oxide film, glucose conversion occurs mostly on the sites where GOx is immobilized, and the resulting GL reacts with APMA subsequently to form GPMAA on the film (Figure 4B). This is consistent with a shift in reaction kinetics from being glucose export-limited in the former case to GOx reaction-limited at the graphene oxide in the latter case. We note that this is not a typical composite to have reinforcement effect; rather, designed for convenient characterization of the hydrogel distinguished from

graphene oxide or GOx. We will see the graphene oxide accelerate hydrogel formation by mixing isolated chloroplasts with the GOx anchored graphene oxide suspension, as shown in Figure 2B.

The characteristic IR peak from the newly formed amide bond in GPMAA hydrogel appears at 1625 cm^{-1} on graphene oxide film (Figure 2A and S10). The increased Raman band at 1245 cm^{-1} is tentatively assigned to v(C-N), δ (NH) in vibrational mode (amide III) (Figure 4C). Mapping of the characteristic Raman bands of GPMAA based on the ratio between two bands at 1245 cm^{-1} and at 1290 cm^{-1} indicates that GPMAA hydrogel forms alongside chloroplast membranes. (Figure 4D, S11-S13). The chloroplasts-embedded GPMAA hydrogel grows slowly, at a rate of 60 μm^3 per chloroplast in very mild conditions and can provide suitable media to maintain the viability of the isolated chloroplasts by entrapment. We postulate that the growing hydrogel protects chloroplast membrane as a physical support and scavenges H_2O_2 generated from glucose oxidation since H_2O_2 can aid polymerization and crosslinking.[47-49] The stability of the embedded chloroplast activity can be a critical factor to maintain the growth rate of this material. In this study, the embedded spinach chloroplasts can be still active for more than 80 h based on our previous study.[43] We expect that the inherent lifetime of isolated chloroplasts is species-dependent, ranging from hours to months.[43,50-51] In addition, we anticipate that if α-glucosidase and glucose dehydrogenase pyrrolo-quinoline quinone could be incorporated in the system to hydrolyze and oxidize maltose,[22] the growing rate of the material would be enhanced due to higher monomer availability.

Characterization of Self-Healing Hydrogel Composite

Physically separated hydrogels are able to seamlessly recombine upon light exposure (**Figure 5**). In the absence of additional GL, the hydrogel shows some repair of fissures but with some defects apparent upon mechanical deformation (Figure 5A), suggesting that the material repair initiates from the external surface. When 5 μL of 1 M GL solution is added to the interface of two physically separated hydrogels, this results in the formation of more extensively repaired gels, which can then sustain more stringent deformation (Figure 5B). As a negative control, we find that separated hydrogels placed together physically but kept in the dark overnight are easily separated by deformation (Figure S14). GPMAA hydrogel forms multiple hydrogen bonds with surrounding water molecules as well as inter-hydrogen bonds between the polymer chains. Hydrogen bonds are one of the common mechanisms used in self-repairing materials.[53] Since UV-irradiation energy is directly absorbed by the glucose moiety, the formation of free radicals can be involved in acrylamide polymerization or hydrogen bonding with hydroxyl groups.[54-56] Physically contacting two GPMAA hydrogels on the face restores the mechanical strength (shear stress) by nearly 50 %, whereas the addition of GL and light exposure allow the restoration of the original mechanical strength (Figure 5C). This demonstration is a mimic of chloroplast embedded-gel matrix that primarily polymerizes and crosslinks by light and continuously grows and self-repairs by the supply of glucose from the atmospheric CO_2 fixation (Figure 5D). This self-healing mechanism is new and different to conventional self-healing relying on non-covalent interactions or specific chemical bonds that form or break reversibly. Glucose molecules supplied by chloroplasts repair the local damage by exceeding its own local material balance through the atmospheric CO_2 fixation.

In summary, we have created a new class of carbon fixating materials that grows, strengthens and self-repairs using ambient solar fluence and atmospheric carbon dioxide. This work highlights how the photosynthetic hydrogel composite systems can be optimized, including productivity and stability of extracted chloroplasts by controlling the illumination period, delivering antioxidant nanoceria inside of chloroplasts, and increasing chloroplast glucose export rate. We note substantial improvement in the mechanical property is needed for the practical use of this self-healing material. Further optimization of the carbon-fixating system and extending the lifetime of the embedded chloroplasts will invariably improve the growing rate and the repair efficiency of the material. We foresee that this class of new materials will find broad utility in fields ranging from biomedicine, material construction, or defense related applications.

Experimental Section

Isolation of chloroplasts: Chloroplasts isolation was performed as previously reported with a slight modification.[57-59] Commercially available fresh baby spinach leaves (*Spinacia oleraceae L.*) were thoroughly washed with de-ionized water and the excess water was removed. After removing the middle veins, the leaves were chopped into small pieces (approximately 0.5 cm × 0.5 cm) and homogenated by blending in HEPES buffer (30 mM, pH 7.6) containing polyethylene glycol (Mw. 8,000, 10% (w/v)),[60] K_3PO_4 (0.5 mM), and $MgCl_2$ (2.5 mM) in an iced bath. The resulting homogenate was filtered through four layers of cheesecloth and the chloroplasts pellet was collected by centrifugation at 4,000 rpm for 15 min at 4 ˚C. The chloroplasts were re-suspended in the aforementioned buffer and added on

top of a 40% Percoll/buffer layer to separate the intact chloroplasts from the broken ones. The intact chloroplasts were sedimented as a pellet whereas the broken chloroplasts form a band in the Percoll layer by centrifugation at 1,700 × *g* for 7 min at 4 ˚C. The upper phases were carefully removed to collect the pellet with intact chloroplasts. This chloroplast pellet was washed with buffer to remove Percoll, and then re-suspended in buffer.

Estimation of chlorophyll concentration: The yield of isolated chloroplasts is estimated by a unit chlorophyll basis (mg of chlorophyll). The chloroplast suspension is diluted by 100 times in 80% acetone and mixed well to dissolve the chloroplast membrane. This suspension is centrifuged for 2 minutes at 3,000 ×g and the supernatant is retained. The absorbance of the supernatant is determined at 652 nm using a Shimadzu UV-3101PC, and then multiplied by the dilution factor (100) followed by dividing by the extinction coefficient of 36 to get the mg of chlorophyll per mL of the chloroplast suspension.

$$\frac{mg\ chlorophyll}{mL} = \frac{A_{652}}{36} \times 100$$

Typical chlorophyll concentrations in this study were 0.90 – 1.14 mg mL^{-1}.

Isolated chloroplasts glucose export: Chloroplasts suspension (10 mL) was placed in a 6 cm-diameter glass petri dish closed with a loose glass lid to allow chloroplasts to capture light and atmospheric carbon dioxide. Chloroplasts were illuminated with a light intensity of approximately 200 µmol m^{-2} s^{-1} photosynthetic active radiation (40 W m^{-2}) using a light-emitting diode flood lamp FL-70W (LED wholesalers).

Glucose concentration is measured by hexokinase since glucose is phosphorylated by adenosine triphosphate (ATP) in the reaction catalyzed by hexokinase.[61-63] Phosphorylated glucose, gluocose-6-phosphate, is then oxidized to 6-phosphogluconate in the presence of oxidized nicotinamide adenine dinucleotide (NAD) in a reaction catalyzed by glucose-6-phosphae dehydrogenase. During the oxidation, an equimolar amount of NAD is reduced to NADH and consequently the absorbance at 340 nm increases, which is directly proportional to glucose concentration. Glucose (HK) assay reagent (Sigma) is prepared, which contains NAD (1.5 mM), ATP (1.0 mM), hexokinase (1.0 U mL^{-1}), and glucose-6-phosphate dehydrogenase (1.0 U mL^{-1}) with preservatives such as sodium benzoate and potassium sorbate. One U is defined as the amount that catalyzes the conversion of 1 micromole of substrate per minute under standard conditions. Glucose solutions in different concentrations are prepared to obtain a standard curve based on the absorbance at 340 nm. Reaction is carried out for 15 minutes at room temperature. The blank accounts for the contribution to the absorbance of the sample and the assay reagents.

$$\mu g \text{ glucose } mL^{-1} = \frac{\Delta A \cdot TV \cdot Mw \cdot F}{\varepsilon \cdot d \cdot SV},$$

where ΔA is difference in absorbance between the sample and the blank, TV is total assay volume (mL), SV is sample volume (mL), Mw is a molecular weight of glucose 180.2 g mol^{-1}, F is dilution factor, ε is extinction coefficient for NADH at 340 nm (mL μM^{-1} cm^{-1}), and d is light path 1 (cm).

The initial glucose concentration from isolated chloroplasts within one hour is determined to be on average approximately 130 µg mg^{-1} Chl. This value is attributed to

previously stored starch inside the chloroplasts and is therefore subtracted to exclusively study glucose export from photosynthesis in isolated chloroplasts. Accordingly, concentration is shown in negative value when glucose influx is higher than glucose export. Although chlorophyll concentration of chloroplast suspension is maintained at approximately 0.1 mg mL^{-1} throughout all experiments, control experiment were performed each time to account for batch-to-batch variability in functioning chloroplasts from each extraction round. The amount of sugar molecules exported from isolated chloroplast has been reported as an accumulated quantity within the first few hours from extraction.[16,32,33,35,64] We mainly discuss glucose concentration measured for 8 h because physical damage in the chloroplast membrane starts being observed after 8 h of incubation at room temperature.

Measurement of gluconolactone: Gluconolactone centration measurement was performed by assay kit (Megazyme Inc., Ireland) and followed the procedure. Gluconolacone (GL) is hydrolyzed in sodium hydroxide solution (2 M, pH 11) at room temperature for 10 min. The resulting gluconic acid is phosphorylated to gluconate-6-phosphate by gluconate kinase and ATP. Gluconate-6-phosphate is converted to ribulose-5-phosphate by 6-phosphogluconate dehydrogenase (6-PDGH) in the presence of nicotinamide-adenine dinucleotide phosphate ($NADP^+$). We measure the absorbance at 340 nm, which is increased by the amount of reduced nicotinamide-adenine dinucleotide phosphate (NADPH) formed in this reaction that is stoichiometric with the amount of gluconic acid. Reaction is carried out for 6 minutes at room temperature. The blank takes into account the contribution to the absorbance of the sample and the assay reagents.

$$\mu g\ GL\ mL^{-1} = \frac{\Delta A \cdot TV \cdot Mw \cdot F}{\varepsilon \cdot d \cdot SV},$$

where ΔA is difference in absorbance between the sample and the blank, TV is total assay volume (mL), SV is sample volume (mL), Mw is a molecular weight of gluconolacone 178.1 g/moL, F is dilution factor, ε is extinction coefficient 6300 for NADPH at 340 nm (L mol^{-1} cm^{-1}), and d is light path 1 (cm).

Nanoceria synthesis: Poly (acrylic acid)-coated nanoceria was synthesized by Asati et al. with some modifications.[65] Cerium (III) nitrate (1 M, 2.5 mL, Sigma Aldrich) and an aqueous solution of poly(acrylic acid) (Mw 1,800, 0.5 M, 2.5 mL, Sigma Aldrich) were added dropwise to HEPBS buffer (0.4 M, 12.5 mL, Sigma Aldrich). The resulting mixture was adjusted to pH 8.5 with NaOH (8 M) and the reaction was continued for 1 day at room temperature under magnetic stirring. The supernatant was collected, concentrated and purified by centrifugation at 4,000 RCF for 10 min using a 10K Amicon centrifugal filter (Millipore Inc.).

Hydrogel synthesis: Gluconolactone (GL) solution was mixed with 3-aminopropyl methacrylamide (APMA) solution in phosphate buffer (pH 7.0) or chloroplast buffer (pH 7.6), and the mixture was placed under the ambient light for overnight at room temperature. GL (1 M) and APMA (1 M) solution were used for in vitro synthesis for characterization. This mixture (70 µL) of GL and APMA was placed on the glass slide and kept under the light in the air after 40 min UV-irradiation at 365 nm (4 W (J s^{-1}), 5.5 cm distance). (UVGL-15, Ultra-Violet Products Let. CA, USA)

Measurement of hydrogel swelling property: Dry hydrogel (80 – 120 mg) was immersed in 50 mL of deionized water for 48 h at room temperature.[66] After swelling, the hydrogel was sediment to separate the insoluble part. The selling was calculated as follows

$$Swelling = \frac{W_s - W_d}{W_d}$$

where, W_s is the weight of hydrogel in swollen state and W_d is the weight of hydrogel in dry state.

Evaluation of rheological properties: Rheological properties of the hydrogels were characterized using Anton Paar MCR-301 rheometer (Anton Paar, Ashlanad, VA, USA) operating under disposable parallel plate geometry (10 nm diameter) at room temperature. We performed dynamic strain sweep (0.1-100% strain at constant 10 rad s^{-1}) to verify the linear viscoelastic regime, and then carry out frequency sweeps between 0.1 and 100 rad s^{-1} at constant 1% strain. Hydrogels are swollen in 100 wt% DI water for 30 min, then loaded onto a sand paper (Grit:P80, Norton Abrasives, Worcester, MA, USA) to avoid slipping. All measurements were run in triplicate and the results are expressed as the average with standard errors.

Evaluation of mechanical property: The mechanical property of the hydrogel was evaluated using 8848 MicroTester (Instron Corp. MA, USA), where two hydrogels physically contacted to each other was pulled apart by shear stress at the rate of 0.04 mm s^{-1}. Two hydrogels were separately formed on each glass slide (15 × 15 × 0.5 mm). As partially formed hydrogels were physically contacted on the face, the hydrogel continued to polymerize and crosslink, resulting in one merged hydrogel between glass slides. The hydrogel was clamped via sticky

tape that tightly glued to the glass slide. The repairing test was carried out in a similar way. Two complete hydrogels were physically contacted on the face, and then mechanical force was applied or they were kept under the illumination after adding GL to the hydrogel interface.

Estimation of glucose concentration near chloroplast membrane: Approximately one chloroplast per 100 μm^3 (V_1) is observed in the microscope images with 0.1 mg Chl mL^{-1} chloroplast suspension. When the mean concentration of glucose measured in the medium is 5 $\mu M\ h^{-1}$, assuming a chloroplasts as a spherical organelle, the concentration of the exported glucose molecules within a 100 nm distance (x) in a 0.01 ms (t) period ($t \approx \frac{x^2}{2D}$, where glucose diffusion coefficient (D) is 5×10^{-6} $cm^2\ s^{-1}$ in water at 25 ˚C; $V_2=\frac{4}{3}\pi(0.1)^3=4\times10^{-3}$ μm^3) is 2.5×10^4 times as concentrated as the mean glucose concentration in the medium, and is therefore estimated to be 125 $mM\ h^{-1}$.

Preparation of hydrogel using chloroplasts on the graphene oxide film: GOx (20 U mL^{-1}) was mixed with graphene oxide solution (0.1 mg mL^{-1}, Graphene Supermarket, NY) for 1 h at room temperature. This mixture is deposited on the amine-functionalized glass slides for 2 h at room temperature, followed by gentle washing with PBS (×3). Freshly isolated chloroplasts are pre-incubated with nanoceria for 3 h at 4 ˚C, and the remained nanoceria was removed by centrifugation at 4000 rpm for 5 min. The resulting chloroplasts were re-suspended (0.1 mg mL^{-1}) in 0.1% APMA containing buffer, and then added on GOx immobilized graphene oxide film, and incubated under the ambient light for 18 h.

Characterization of hydrogel (FT-IR spectroscopy): Characteristic peaks of functional groups were confirmed by Fourier transform infrared (FT-IR) spectroscopy (Thermo Electron Co. WI, USA).

Characterization of hydrogel within chloroplasts suspension (FT-IR spectroscopy): Characteristic peaks of functional groups were confirmed by FT-IR spectroscopy (FTIR6700 Thermo Fisher Continuum FT-IR microscope). FT-IR spectra were collected from spot size 100×100 μm.

Characterization of hydrogel within chloroplasts suspension (Raman spectroscopy mapping): Raman spectroscopy maps were collected in a confocal Raman spectrometer HR-800 (Horiba BY) using a 632 nm laser source with a 100x objective.

Supporting Information

Supporting Information is available from the Wiley Online Library.

Acknowledgements

The authors acknowledge funding from the Department of Energy, Basic Energy Sciences (DE-FG02-08ER46488). The authors are grateful for helpful discussion with D. Parviz.

Received: ((will be filled in by the editorial staff))
Revised: ((will be filled in by the editorial staff))
Published online: ((will be filled in by the editorial staff))

References

[1] J. A. Syrett, C. R. Becer, D. M. Haddleton, *Polymer Chemistry* **2010**, *1*, 978.

[2] D. Y. Wu, S. Meure, D. Solomon, *Progress in Polymer Science* **2008**, *33*, 479.

[3] C. E. Diesendruck, N. R. Sottos, J. S. Moore, S. R. White, *Angewandte Chemie International Edition* **2015**, *54*, 10428.

[4] X. Chen, M. A. Dam, K. Ono, A. Mal, H. Shen, S. R. Nutt, K. Sheran, F. Wudl, *Science* **2002**, *295*, 1698.

[5] S. D. Bergman, F. Wudl, *Journal of Materials Chemistry* **2007**, *18*, 41.

[6] L. Li, B. Yan, J. Yang, L. Chen, H. Zeng, *Advanced Materials* **2015**, *27*, 1294.

[7] A. Phadke, C. Zhang, B. Arman, C.-C. Hsu, R. A. Mashelkar, A. K. Lele, M. J. Tauber, G. Arya, S. Varghese, *Proc. Natl. Acad. Sci. U.S.A.* **2012**, *109*, 4383.

[8] M. Nakahata, Y. Takashima, H. Yamaguchi, A. Harada, *Nat Commun* **2011**, *2*, 511.

[9] A. Harada, Y. Takashima, M. Nakahata, *Acc. Chem. Res.* **2014**, *47*, 2128.

[10] S. C. Grindy, R. Learsch, D. Mozhdehi, J. Cheng, D. G. Barrett, Z. Guan, P. B. Messersmith, N. Holten-Andersen, *Nature Materials* **2015**, *14*, 1210.

[11] S. Srivastava, M. Andreev, A. E. Levi, D. J. Goldfeld, J. Mao, W. T. Heller, V. M. Prabhu, J. J. de Pablo, M. V. Tirrell, *Nat Commun* **2017**, *8*, 14131.

[12] S. R. White, N. R. Sottos, P. H. Geubelle, J. S. Moore, *Nature* **2001**, 409, 794.

[13] S. H. Cho, H. M. Andersson, S. R. White, N. R. Sottos, P. V. Braun, *Advanced Materials* **2006**, *18*, 997.

[14] K. S. Toohey, N. R. Sottos, J. A. Lewis, J. S. Moore, S. R. White, *Nature Materials* **2007**, *6*, 581.

[15] S. Gupta, S. D. Pang, H. W. Kua, *Construction and Building Materials* **2017**, *146*, 419.

[16] S. E. Weise, A. P. M. Weber, T. D. Sharkey, *Planta* **2004**, *218*, 474.

[17] K. Kobayashi, H. Sumitomo, Y. Ina, *Polymer Journal* **1983**, *15*, 667.

[18] R. P. Wool, *Soft Matter* **2008**, *4*, 400.

[19] J. S. Dordick, R. J. Linhardt, D. G. Rethwisch, *Chemtech* **1994**, *24*, 33.

[20] Q. Wang, J. S. Dordick, R. J Linhardt, *Chem. Mater.* **2002**, *14*, 3232.

[21] T. Yamada, H. Arakawa, T. Okajima, T. Shimada, A. Ikai, *Ultramicroscopy* **2002**, *91*, 261.

[22] H. Zhang, D. Zhai, Y. He, *RSC Adv.* **2014**, *4*, 44600.

[23] H.-P. Cong, P. Wang, S.-H. Yu, *Chem. Mater.* **2013**, *25*, 3357.

[24] M. A. Rafiee, J. Rafiee, Z. Wang, H. Song, Z.-Z. Yu, N. Koratkar, *ACS Nano* **2009**, *3*, 3884.

[25] S. Alwarappan, C. Liu, A. Kumar, C.-Z. Li, *The Journal of Physical Chemistry C* **2010**, *114*, 12920.

[26] G. Ritte, K. Raschke, *New Phytologist* **2003**, *159*, 195.

[27] D. A. Walker, *Photosynth Res* **2003**, *76*, 319.

[28] D. Joly, R. Carpentier, *Methods Mol. Biol.* **2011**, *684*, 321.

[29] S. P. Robinson, D. A. Walker, *FEBS Lett.* **1979**, *107*, 295.

[30] G. Schäfer, U. Heber, *Plant Physiology* **1977**, *60*, 286.

[31] D. G. Peavey, M. Steup, M. Gibbs, *Plant Physiology* **1977**, *60*, 305.

[32] M. Stitt, H. W. Heldt, *Plant Physiology* **1981**, *68*, 755.

[33] H. E. Neuhaus, N. Schulte, *Biochemical Journal* **1996**, *318 (Pt 3)*, 945.

[34] N. J. Kruger, T. A. Rees, *Planta* **1983**, *158*, 179.

[35] J. C. Servaites, D. R. Geiger, *J Exp Bot* **2002**, *53*, 1581.

[36] U. Heber, J. Viil, S. Neimanis, T. Mimura, K. J. dietz, *zeitschrift fur naturforschung C-A journal of biosciences* **1989**, *44c*, 524.

[37] I. M. Rao, N. Terry, *Plant Physiology* **1989**, *90*, 814.

[38] R. K. Monson, M. E. Rumpho, G. E. Edwards, *Planta* **1983**, *159*, 97.

[39] W. Cockburn, C. W. Baldry, D. A. Walker, *Biochimica et Biophysica Acta (BBA) - Bioenergetics* **1967**, *131*, 594.

[40] U. I. Flugge, M. Freisl, H. W. Heldt, *Plant Physiology* **1980**, *65*, 574.

[41] P. E. Giebel, *Extraction of Chloroplasts from Plant Tissue and Their Use in Demonstrating the Hill reaction,* Dept. of Biol. Virginia Commonwealth Univ., Richmond, VA, **2006**. 31-47.

[42] J. C. Rooke, C. Meunier, A. Léonard, B.-L. Su, *Pure and Applied Chemistry* **2008**, *80*, 1249.

[43] A. A. Boghossian, F. Sen, B. M. Gibbons, S. Sen, S. M. Faltermeier, J. P. Giraldo, C. T. Zhang, J. Zhang, D. A. Heller, M. S. Strano, *Advanced Energy Materials* **2013**, *3*, 881.

[44] J. P. Giraldo, M. P. Landry, S. M. Faltermeier, T. P. McNicholas, N. M. Iverson, A. A. Boghossian, N. F. Reuel, A. J. Hilmer, F. Sen, J. A. Brew, M. S. Strano, *Nature Materials* **2014**, *13*, 400.

[45] Y. Nakano, K. Asada, *Plant Cell Physiol* **1980**, *21*, 1295.

[46] P. W. Barone, S. Baik, D. A. Heller, M. S. Strano, *Nature Materials* **2005**, *4*, 86.

[47] A. Elgawish, M. Glomb, M. Friedlander, V. M. Monnier, *J. Biol. Chem.* **1996**, *271*, 12964.

[48] J. H. Baxendale, M. G. Evans, C. S. Park, *Trans. Faraday Soc.* **1946**, *42*, 155.

[49] U. S. Nandi, S. R. Palit, *Journal of Polymer Science Part A: Polymer Chemistry* **1955**, *17*, 65.

[50] R. K. Trench, J. E. Boyle, D. C. Smith, *Proceedings of the Royal Society B: Biological Sciences* **1973**, *184*, 51.

[51] B. J. Green, W.-Y. Li, J. R. Manhart, T. C. Fox, E. J. Summer, R. A. Kennedy, S. K. Pierce, M. E. Rumpho, *Plant Physiology* **2000**, *124*, 331.

[52] S. Igarashi, T. Ohtera, H. Yoshida, A. B. Witarto, K. Sode, *Biochemical and Biophysical Research Communications* **1999**, *264*, 820.

[53] L. Brunsveld, B. Folmer, E. W. Meijer, R. P. Sijbesma, *Chem. Rev.* **2001**, *101*, 4071.

[54] H. Kashiwagi, S. Enomoto, *Chem. Pharm. Bull.* **1981**, *29*, 913.

[55] H. Ueda, Z. Kuri, S. Shida, *Nippon kagaku zassi* **1961**, *82*, 8.

[56] M.-X. Fu, K. J. Wells-Knecht, J. A. Blackledge, T. J. Lyons, S. R. Thorpe, J. W. Baynes, *Diabetes* **1994**, *43*, 676.

[57] S. P. Robinson, *Photosynth Res* **1983**, *4*, 281.

[58] R. M. Lilley, M. P. Fitzgerald, K. G. Rienits, D. A. Walker, *New Phytologist* **1975**, *75*, 1.

[59] D. I. Arnon, *Plant Physiology* **1949**, *24*, 1.

[60] B. E. Michel, M. R. Kaufmann, *Plant Physiology* **1973**, *51*, 914.

[61] R. J. Bondar, D. C. Mead, *Clinical Chemistry* **1974**, *20*, 586.

[62] R. Geiger, H. Fritz, *Methods of Enzymatic Analysis*, Edited by Bergmeyer, **1984**.

[63] D. Southgate, *Measurement of Unavailable Carbohidrates. Structural and Non-Structural Polysaccharides, in." Determination of Food Carbohydrate" Dat Southgate, Ed*, **1976**.

[64] H. W. Heldt, C. J. Chon, D. Maronde, A. Herold, Z. S. Stankovic, D. A. Walker, A. Kraminer, M. R. Kirk, U. Heber, *Plant Physiology* **1977**, *59*, 1146.

[65] A. Asati, S. Santra, C. Kaittanis, J. M. Perez, *ACS Nano* **2010**, *4*, 5321.

[66] N. Nagasawa, T. Yagi, T. Kume, F. Yoshii, *Carbohydrate Polymers* **2004**, *58*, 109.

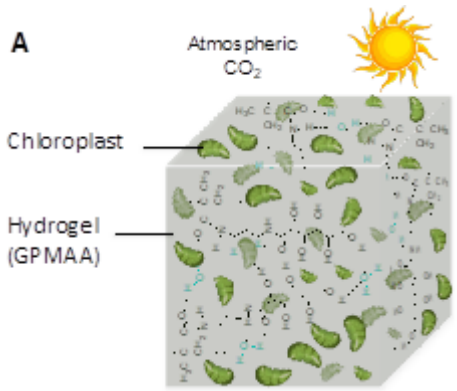

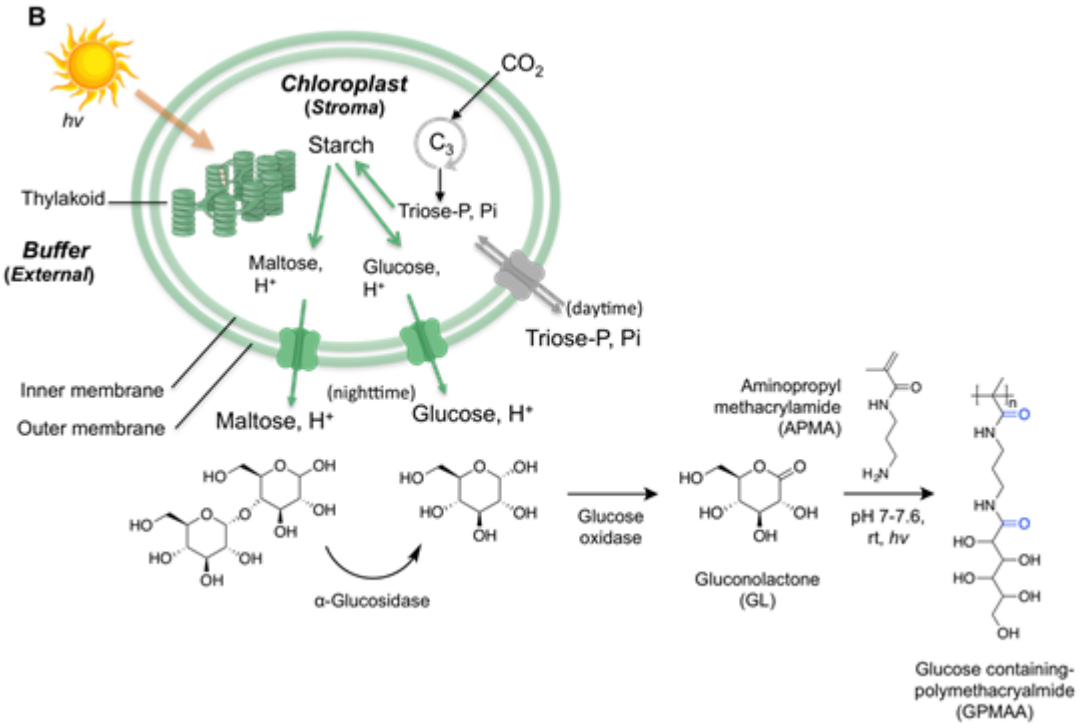

Figure 1. A schematic illustration of a synthetic material that grows, strengthens and self-repairs with embedded plant chloroplasts. (A) GPMAA forms hydrogel as lightly cross-linked by hydrogen bonding in water. The hydrogel continuously grows, strengthens and self-repairs as long as chloroplasts carry out carbon fixation and export glucose. **(B)** Chloroplasts transform solar energy and carbon dioxide into the chemical energy and the assimilated carbon in the form of triose phosphate during the day. Alternatively, chloroplasts export maltose and glucose resulting from the breakdown of starch through the translocators at night. Exported glucose and glucose from enzymatic hydrolysis of maltose are converted to gluconolactone (GL) by GOx, and subsequently react to primary amine functionalized methacrylamide (APMA) and polymerize to glucose-containing polymethacryamide (GPMAA) in the medium.

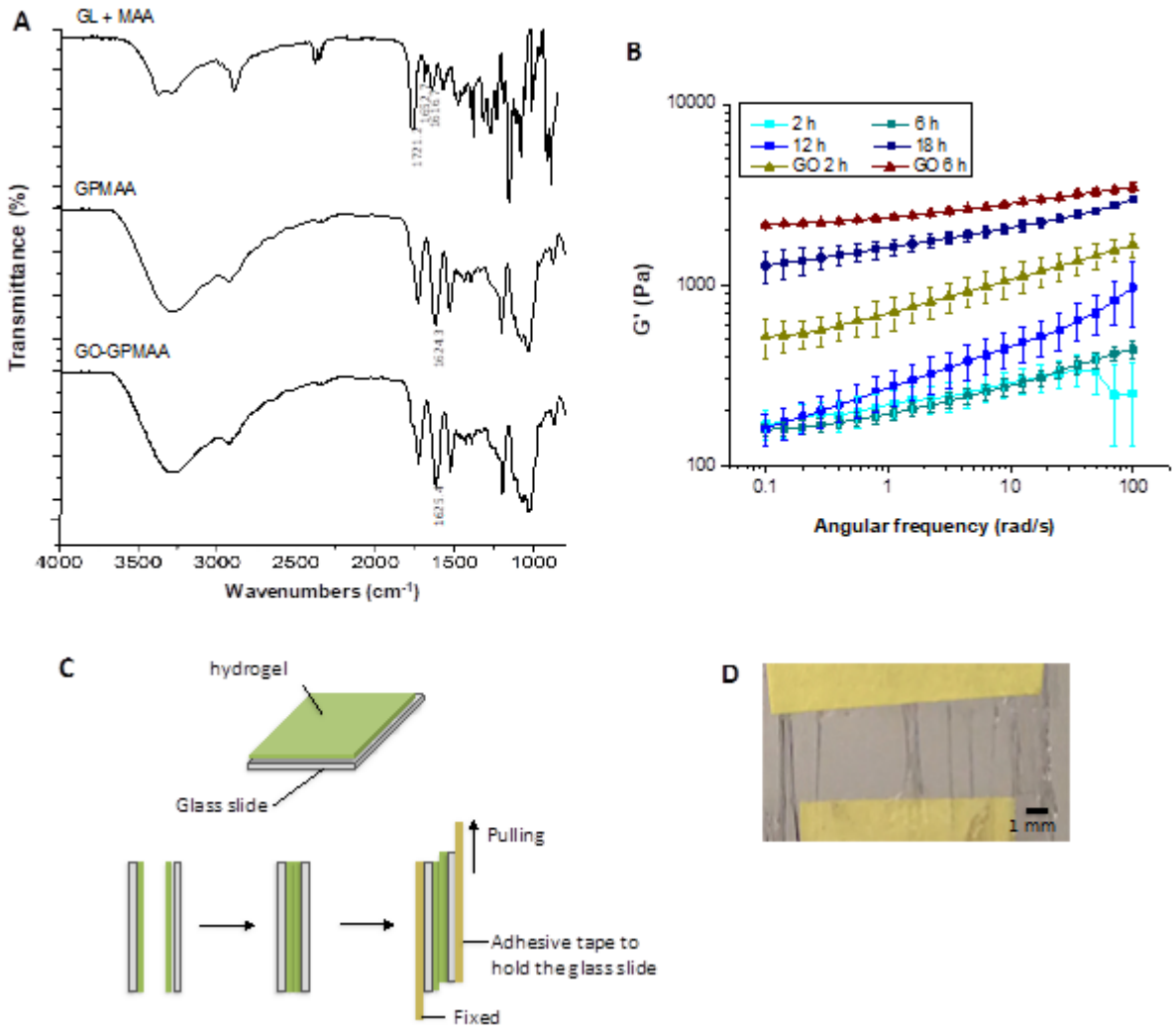

Figure 2. In vitro a carbon fixing hydrogel formation from gluconolactone and 3-aminopropyl methacrylamide. (A) FT-IR spectra of the mixture of GL and APMA at 0 h, GPMAA and GO-GPMAA in 5 h under the light, (B) Rheology properties of GPMAA (squares) and graphene oxide (GO) containing GPMAA (triangles) at different reaction time. The data are expressed as the average ±SD (n=3), (C) a schematic illustration on separation of GPMAA hydrogel, (D) Formation of fibrillar structure during the separation process, Two separated thin GPMAA hydrogels are formed on the glass slides and then they are attached to each other. The glass slides are pulled separating the hydrogels at a rate of 0.04 mm/sec.

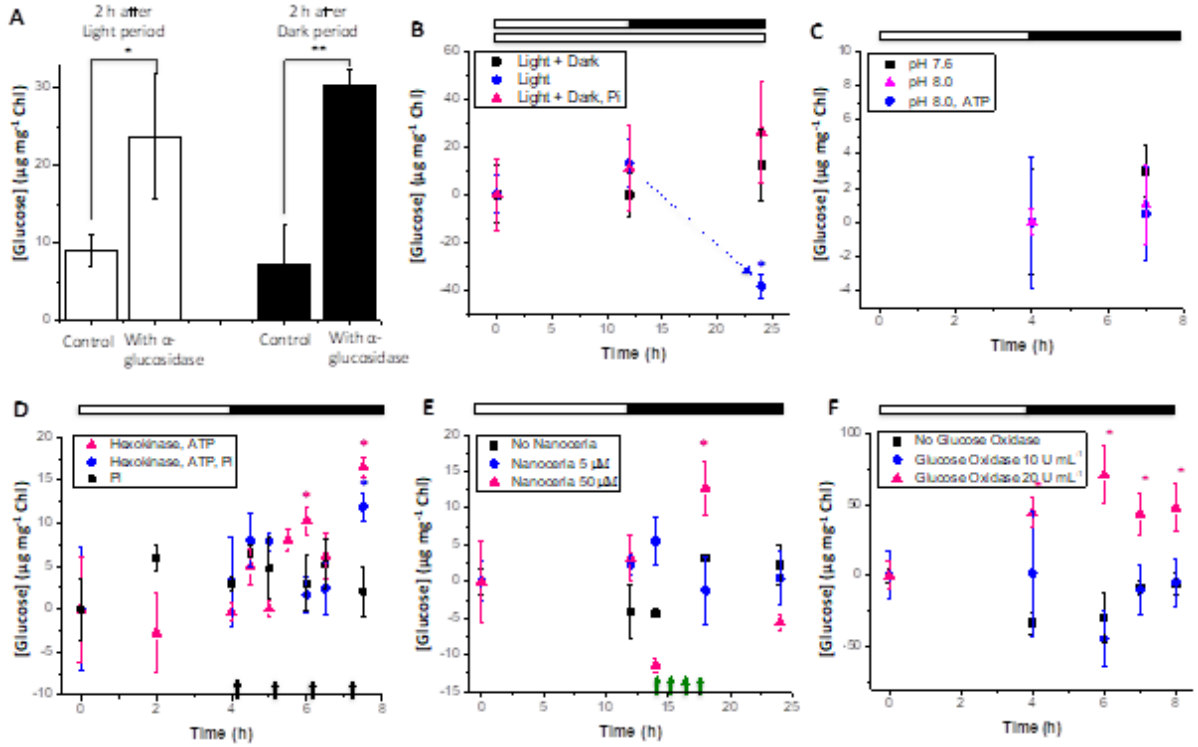

Figure 3. Systematic investigation on boosting glucose synthesis and export from isolated chloroplast. (A) Glucose concentration with and without maltose hydrolysis by a-glucosidase (24 U mL^{-1}) at light and dark period. Total incubation time is 8 h with 4 h of light and 4 h of dark, (B) Glucose concentration in different illumination time; 12 h light and 12 h dark (black squares), continuous illumination for 24 h (blue circles), and 12 h light and 12 h dark with 5 mM Pi supply at the beginning of dark period (pink triangles), (C) Effect of chloroplast proton gradient or ATP on glucose export. Chloroplast medium is adjusted from optimum pH 7.6 (control, black squares) to pH 8.0 (pink triangles) to induce alkalinization of chloroplast stroma, and 2 mM ATP is added to the medium (blue circles) to enhance active transport mechanism of glucose, (D) Comparison of approaches to boost glucose export under presence or absence of external Pi supply. A mixture of hexokinase (10 U mL^{-1}), 0.6 mM ATP, with 5 mM Pi (blue circles) or without additional Pi (pink triangles), or 5 mM Pi alone (black squares) is added to the chloroplast suspension medium at every hour during the dark period. Black arrows indicate the addition of 5 mM Pi, (E) Effect of nanoceria on glucose export after 12 h light period. Chloroplasts are incubated in presence of nanoceria 3 h prior to the light period. Final concentration of nanocrea is 5 µM (blue circles) or 50 µM (pink triangles). Control means chloroplast incubated for the experimental period without nanoceria (black squares). Green arrows indicate the addition of hexokinase reaction mixture. White or black rectangles on the top of each graph imply light or dark period, respectively, (F) GL concentration from chloroplasts incubated in the medium containing 20 U mL^{-1} GOx under the continuous illumination for 5 h. White or black rectangles on the top of each graph imply light or dark period, respectively. GL concentration is presented by gluconic acid after

hydrolysis in 2M NaOH. The data are expressed as the average ±S.D. (n=5-10). *P, **P<0.05 compared with control [Glucose] at 0 h.

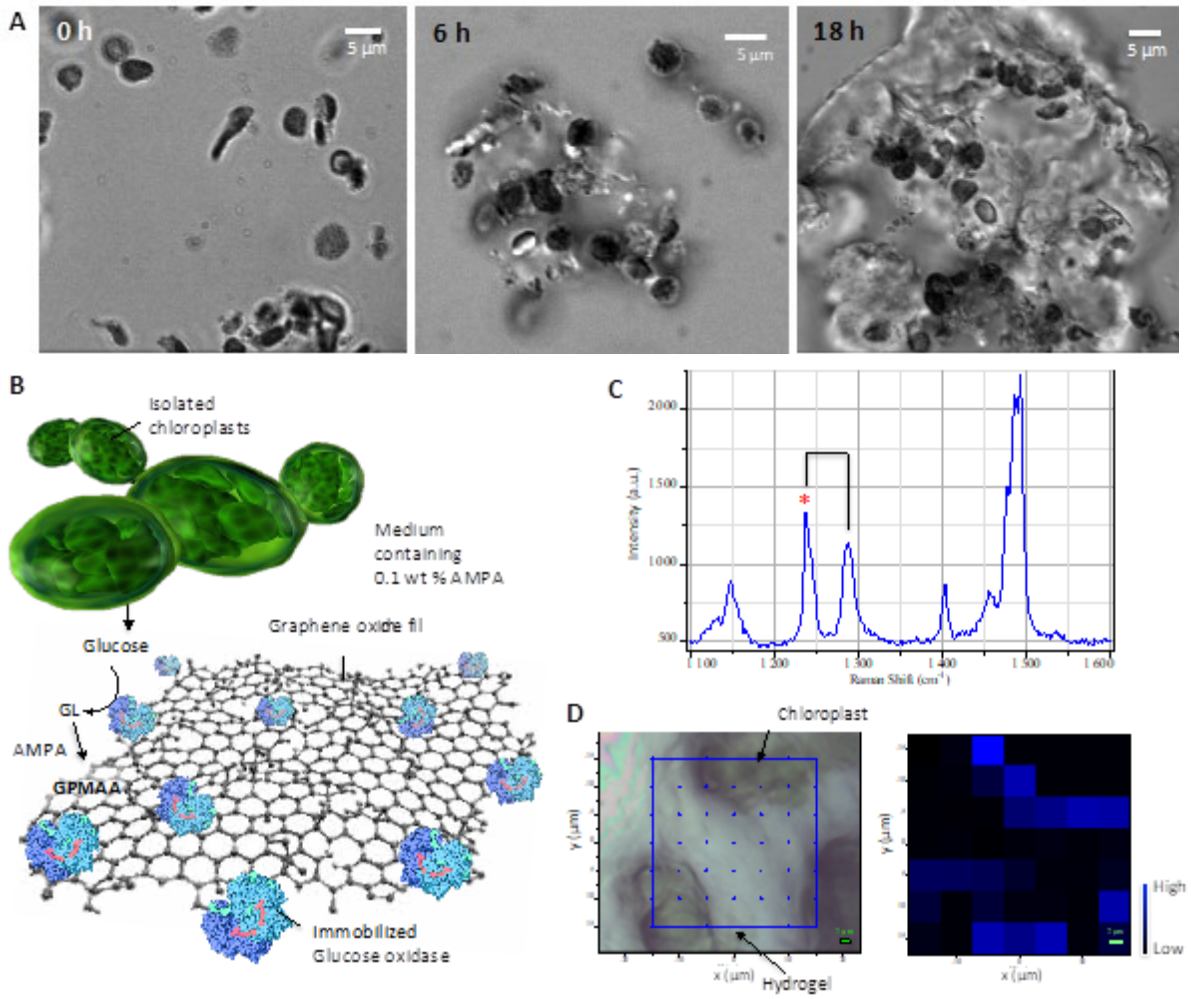

Figure 4. Hydrogel growth over time from ambient carbon dioxide and light around isolated chloroplasts. (A) Microscope images of growing hydrogel near the isolated chloroplasts in the medium containing GOx (20 U mL^{-1}) and 0.1% w/v APMA. Exposure conditions are ambient CO_2 and 18 h ambient illumination after 1 h dark period. Scale bars are 5 µm, (B) Schematic illustration of hydrogel formation on the graphene oxide film. Isolated chloroplasts are incubated with GOx immobilized graphene oxide film in the medium containing 0.1% APMA. Followed by glucose export from chloroplasts, glucose is converted into GL on the graphene oxide surface by GOx followed by reacting to APMA, which polymerizes to form GPMAA, (C) Characteristic Raman bands of GPMAA hydrogel, (D) Optical image of chloroplast embedded-GPMAA hydrogel (left) and Raman mapping (right) based on the

characteristic Raman bands ratio between 1245 and 1290 cm^{-1} under a laser excitation of 632 nm. Scale bars are 2 μm.

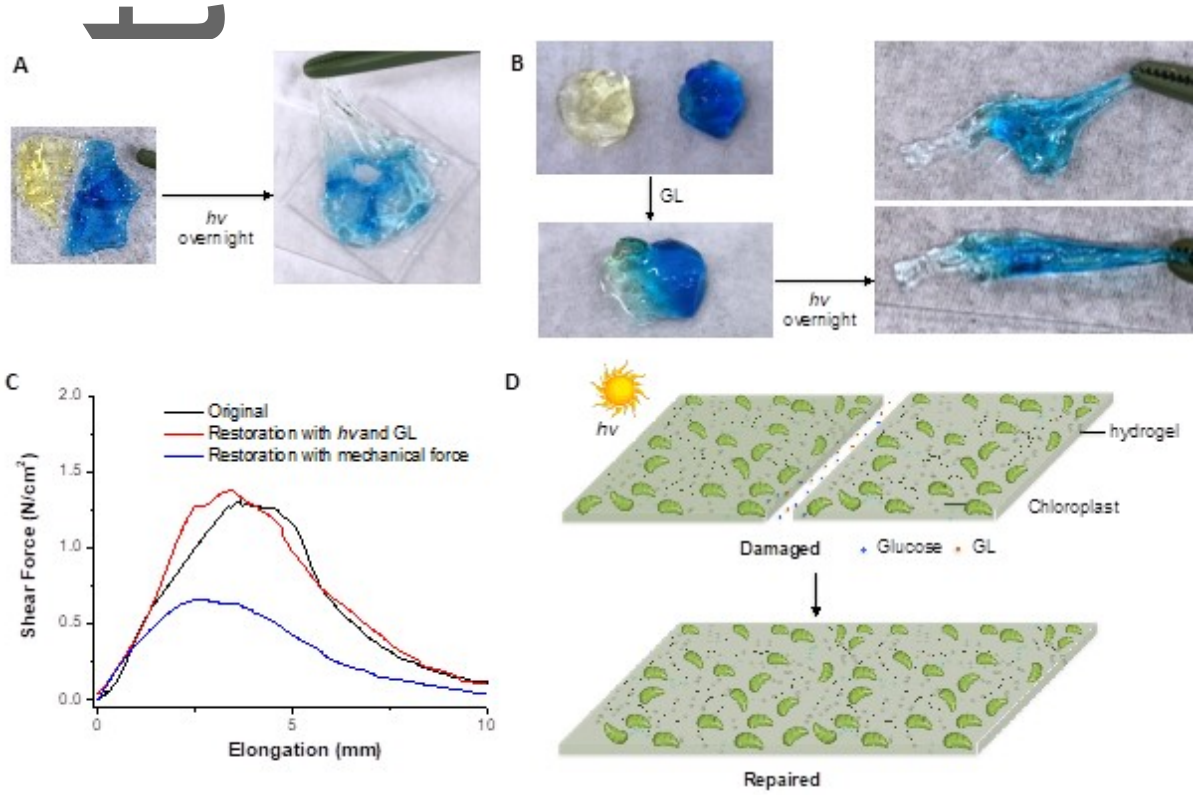

Figure 5. Self-repair property of GPMAA hydrogel. (A) Partially repaired hydrogels by exposure to light overnight, hydrogels are dyed yellow and blue to allow for easily distinguished interface, (B) Fully repaired hydrogels by addition of 1 M GL (5 μL) to the interface and exposure to light overnight, (C) Shear strength restoration of hydrogels by physical attachment for 30 min (blue line) or exposure to light overnight after addition of GL (red line). Two separated thin GPMAA hydrogels are formed on the glass slides and then they are attached to each other. The glass slides are pulled separating the hydrogels at a rate of 0.04 mm/sec. (D) Schematic illustration of self-healing mechanism of chloroplast embedded hydrogel matrix. Glucose molecules supplied by chloroplasts repair the local damage by exceeding its own local material balance through the atmospheric CO_2 fixation.

Carbon fixating materials is created that grow, strengthen and self-repair using ambient solar fluence and atmospheric CO_2. This system contains aminopropyl methacrylamide, glucose oxidase and nanoceria stabilized-extracted chloroplasts and generates hydrogels with 3 kPa shear modulus at a growth rate of 60 $\mu m^3\ h^{-1}$ per chloroplast by insertion of chemoprotective nanoceria inside chloroplasts and systemic optimization of glucose efflux rate.

Keyword: carbon-fixating material, chloroplast-embedded hydrogel, self-repair material, ambient CO_2 fixation, polymethyacrylamide and carbon composites

S.-Y. Kwak, J.P. Giraldo, T.T.S. Lew, M.H. Wong, P. Liu, Y.J. Yang, V.B. Koman, M.K. McGee, B.D. Olsen, M.S. Strano*

Polymethacrylamide and Carbon Composites that Grow, Strengthen and Self-Repair using Ambient Carbon Dioxide Fixation